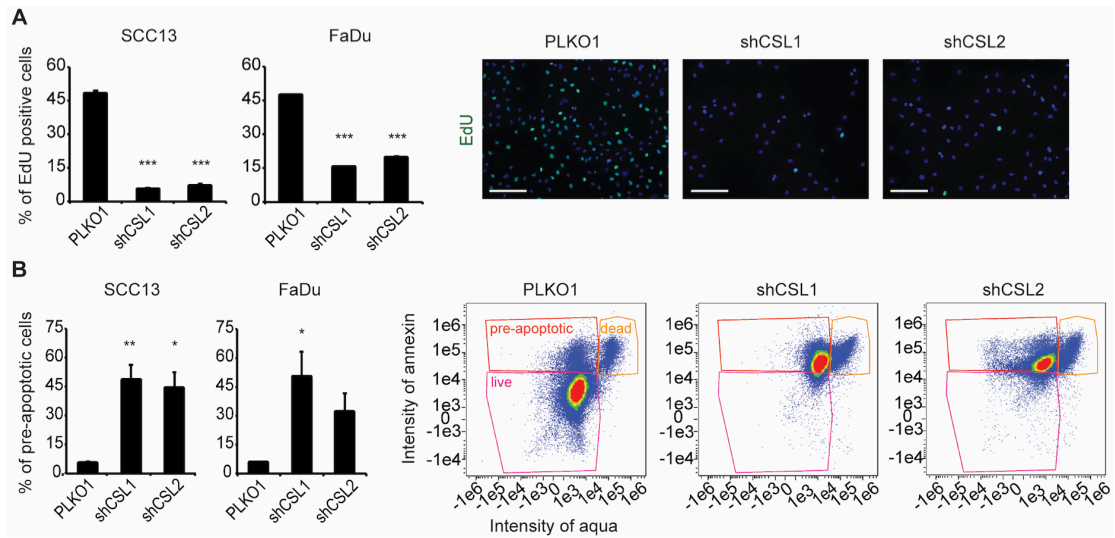
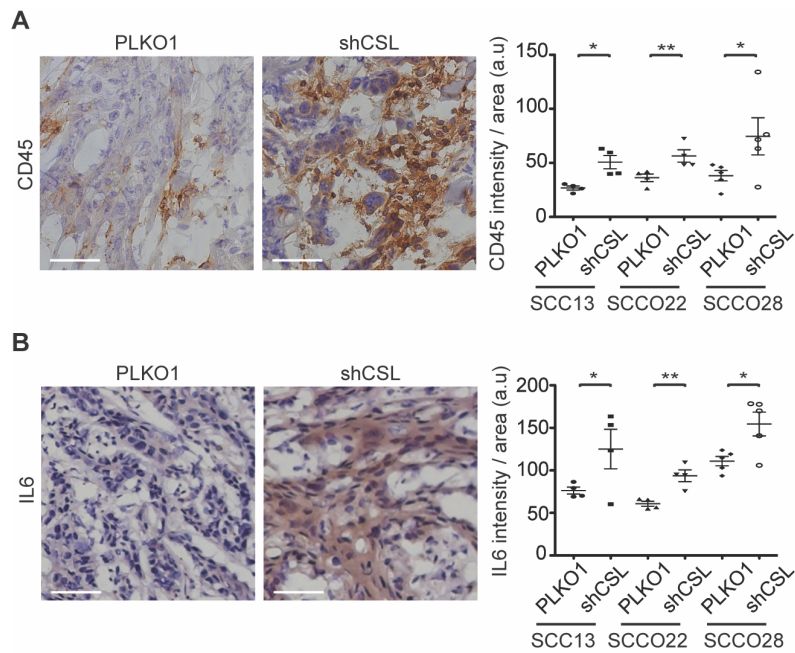


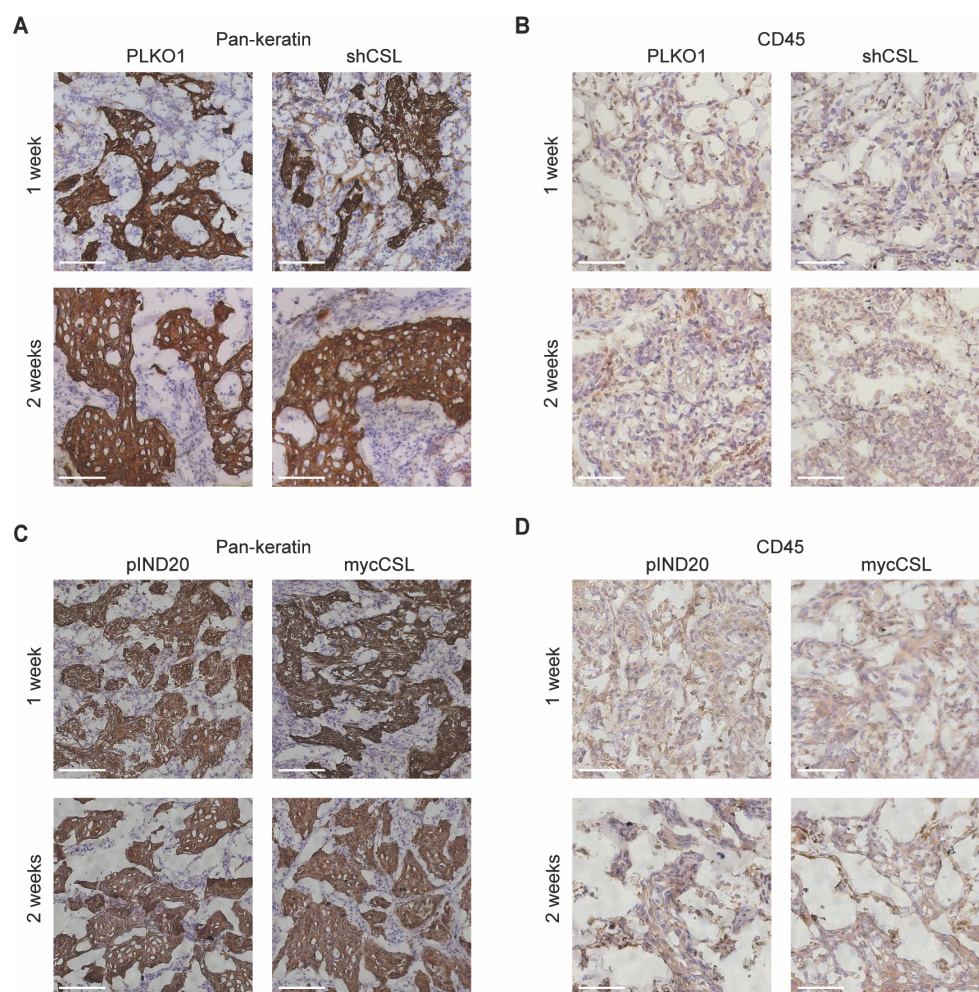
Supplemental Figure 1. Higher CSL expression in proliferating vs. differentiating keratinocytes and in premalignant and malignant neoplastic lesions. **(A)** Immunofluorescence analysis of CSL expression in normal skin from two other individuals besides the one analysed in Figure 1A. Scale bars: 25 μ m. **(B)** Immunohistochemical analysis of CSL expression in four other AK lesions versus corresponding flanking normal (N) skin, besides the one shown in Figure 1C. Scale bars: 100 μ m. **(C)** Immunohistochemical analysis of CSL expression in six other oral SCC lesions besides those shown in Figure 1D, together with flanking dysplastic and N tissues as indicated. Scale bars: 25 μ m. **(D)** Immunoblot analysis of CSL expression in two other HKC strains besides the ones shown in Figure 2A, under proliferating versus differentiating conditions. Numbers refer to relative folds of CSL expression using actin for normalization. **(E)** HKCs as in **D** were analysed by RT-qPCR for CSL mRNA expression with 36B4 for normalization. **(F)** Immunohistochemical analysis of CSL expression in HKC and SCC13 cells. Right panel: quantification of CSL signal intensity using ImageJ software. Scale bars: 100 μ m.



Supplemental Figure 2. Positive role of CSL in promoting proliferative potential and cell survival of SCC cells. **(A)** SCC13 and FaDu cells, infected with two shRNA lentiviruses against CSL, were labeled with EdU for 6 hours. EdU positive cells were counted using ImageJ software analysis. Shown are representative images of FaDu cells. Scale bars: 150 μ m. **(B)** SCC13 and FaDu cells as in **A** were labeled with Annexin-V dye, followed by quantification of positive signal using ImageStream flow cytometer. **(A, B)** Mean \pm s.e.m, one-way Anova with Dunnett test; $n = 3$ independent experiments; * $P < 0.05$, ** $P < 0.005$, *** $P < 0.0005$.



Supplemental Figure 3. Increased inflammation in tumors formed by SCC cells with CSL gene silencing. **(A and B)** Same SCC lesions as in Figure 6 were analysed for CD45 leukocyte and IL6 cytokine marker expression by immunohistochemical staining. Shown are representative images as well as quantification of positive regions using ImageJ software. Scale bars: 250 μ m. Mean \pm s.e.m, one-tailed paired *t*-test; n= 4 mice for SCC13 lesions, n= 4 mice for SCCO22 lesions, and n= 5 mice for SCCO28 lesions; **P*<0.05, ***P*<0.005.



Supplemental Figure 4. Histological features and inflammation in matrigel nodules formed by SCC cells with CSL gene modulation. **(A and B)** Same SCC nodules as in Figure 8A were analyzed for epithelial (Pan-keratin) and leukocyte (CD45) marker expression by immunohistochemical staining. Shown are representative images from week one and two time points. Scale bars: 250 μ m. **(C and D)** Same SCC nodules as in Figure 8D were analyzed for epithelial (Pan-keratin) and leukocyte (CD45) marker expression by immunohistochemical staining. Shown are representative images from week one and two time points. Scale bars: 250 μ m.

Supplemental Table 1. List of genes up/down- modulated by CSL silencing in HKC and SCC cells from RNA-Seq experiment; Gene Ontology of modulated genes.

Supplemental Table 2. List of gene sets from the Molecular Signature Database used for Gene set enrichment analysis of RNA-Seq expression profiles of HKC and SCC13 cells with CSL silencing.

Supplemental Table 3. List of ChIP-Seq peaks in HKCs identified by CSL antibody.

Supplemental Table 4. List of primers used in this study.

Supplemental Table 5. List of antibodies used in this study.